Chemical Physics Letters 576 (2013) 1–9

Contents lists available at SciVerse ScienceDirect

Chemical Physics Letters

journal homepage: www.elsevier.com/locate/cplett

FRONTIERS ARTICLE

Optically induced current in molecular conduction nanojunctions with semiconductor contacts

Boris D. Fainberg [a,b], Tamar Seideman [c,*]

[a] Faculty of Science, Holon Institute of Technology, 58102 Holon, Israel
[b] School of Chemistry, Tel-Aviv University, 69978 Tel-Aviv, Israel
[c] Department of Chemistry, Northwestern University, Evanston 60208, IL, USA

ARTICLE INFO

Article history:
Available online 25 March 2013

ABSTRACT

We propose a new approach to coherent control of transport via molecular junctions, which bypasses several of the hurdles to experimental realization of optically manipulated nanoelectronics noted in the previous literature. The method is based on the application of intrinsic semiconductor contacts and optical frequencies below the semiconductor bandgap. To explore the coherently controlled electronic dynamics, we introduce a density matrix formalism that accounts for both the discrete molecular state and the semiconductor quasicontinua within a single master equation and offers analytically soluble limits for a single and two-site molecular bridge. Our analytical theory predicts a new phenomenon, referred to as coherent destruction of induced tunnelling, which extends the phenomenon of coherent destruction of tunnelling frequently discussed in the previous literature. Our results illustrate the potential of semiconductor contacts in coherent control of photocurrent.

1. Introduction

The field of molecular-scale electronics has been rapidly advancing over the past two decades, both in terms of experimental and numerical technology and in terms of the discovery of new physical phenomena and realization of new applications (for recent reviews please see Refs. [1–3]). In particular, the optical response of nanoscale molecular junctions has been the topic of growing experimental and theoretical interest in recent years [4–15], fueled in part by the rapid advance of the experimental technology and in part by the premise for long range applications in optoelectronics. The ultimate goal of controlling electric transport with coherent light, however, has proven challenging to realize in the laboratory. One difficulty that has been noted in the previous literature is substrate-mediated processes. Light shining on a molecular system in contact with a metal substrate is adsorbed by the substrate, rather than by a molecular bond or the molecule–surface bond in the vast majority of cases, leading to the excitation of hot carriers. The latter may interact with the molecule and lead to interesting dynamics, but in the process coherence is lost. Other competing processes include heating of the electrodes (one of which often consists of an STM tip) and undesired energy transfer events.

Ref. [13] proposes the use of semiconducting electrodes and sub-bandgap frequencies to circumvent undesired substrate-mediated and heating processes. Here, an ultrafast, nanoscale molecular switch is introduced, consisting of a conjugated organic molecule adsorbed onto a semiconducting surface and placed near a scanning tunneling microscope tip. A low-frequency, polarized laser field is used to switch the system by orienting the molecule with the field polarization axis, enabling conductance. Plasmon enhancement and spatial localization of the incident field by the metallic tip allow operation at low laser intensities [13]. Semiconducting electrodes have been used in the experimental literature in the context of a single-quantum-dot photodiode that may be considered as a quantum dot-based junction [16,17]. In addition to introducing a new opportunity for coherent control of transport via junctions, semiconductor-based molecular electronics offer potentially several other attractive properties. From a chemical perspective, organic molecules typically form much stronger bonds with semiconducting surfaces, such as doped silicon, than with metals. From a technological perspective, the addition of molecular function to the already established silicon-based technology is vastly more viable than replacing silicon by metal-based electronics.

Here we propose and explore theoretically a new approach to coherent control of electric transport via semiconducting junctions, which is similar to the concept introduced in Ref. [13] in capitalizing on the use of sub-bandgap frequencies, but is complementary in application. Our approach is based on the excitation of dressed states of the junction Hamiltonian that can be frequency-tuned to tunnel selectively into either the left or the right contacts, thus

---

* Corresponding author. Fax: +1 847 491 7713.
E-mail address: seideman@chem.northwestern.edu (T. Seideman).

0009-2614/$ - see front matter © 2013 Elsevier B.V. All rights reserved.
http://dx.doi.org/10.1016/j.cplett.2013.02.045

generating unidirectional current whose temporal characteristics are controlled by the light pulse.

The next section provides a qualitative discussion of the concept underlying the control mechanism and in Section 3 we develop the theory. In Sections 4 and 5 we address the specific cases of a single- and a double-site bridge (Sections 4 and 5, respectively), both of which are analytically soluble, hence providing useful insights. In particular, our analytical theory extends the phenomenon of coherent destruction of tunneling (CDT) to the light induced case. The final section concludes with a discussion of the implications of our analytically soluble models and a brief outline of other potential avenues for coherent control of transport via semiconductor-based junctions.

2. Control concept

We consider a molecular junction consisting of a molecular moiety that possess a permanent dipole moment **D** and is in contact with two intrinsically semiconducting electrodes. The use of SC contacts circumvents energy transfer from the bridge to the contacts [16], a complicating feature in junctions with metallic contacts, since, as noted above, sub-bandgap light cannot excite electron–hole pairs in a semiconductor substrate [13]. Hence, the main source of relaxation in SC-molecule-SC junctions under the conditions considered is the charge transfer between the bridge and the contacts. The interaction of a nonresonant electromagnetic (EM) field with such systems leads to modulation of their energetic spectrum by the field frequency ω[18–21]. The efficiency of the energy spectrum modulation depends on the interaction parameter $z = \mathbf{D}\cdot\mathbf{E}_0/(\hbar\omega)$, where $\mathbf{E}_0$ is the amplitude of the electromagnetic field $\mathbf{E}(t)$. The permanent dipole moment of relevant molecules can reach 10 D and more. The spectral modulation alters the arrangement of molecular electronic states and may substantially change the electron and hole transfer rates between the molecular bridge and the SC contact, due to the strong dependence of these rates on the position of the molecular level relative to the conduction band (CB) and valence band (VB). Suppose that initially a single molecular level of energy ε_i is positioned between the conduction and valence bands of the SC contacts shown in Fig. 1. No current in such SC-molecule-SC junction is possible even in the presence of the voltage bias. If, however, an electromagnetic pulse of appropriate frequency ω excites the molecular bridge, photonic 'replication' of state i with energy $\varepsilon_i + \hbar\omega$ can be tuned to be close to the CB, while the photonic 'replication' with energy $\varepsilon_i - \hbar\omega$ is energetically close to the VB. In that situation a current flows through the junction and its temporal duration is controlled by the electromagnetic pulse characteristics. The transport rate is largely controlled by the applied voltage bias, which determines the barrier width (the asymmetric case, where the molecular level is remote from the gap center, and/or several levels contribute to the transport, is addressed below). This control enables us to realize coherent excitation of a molecular bridge while circumventing competing processes. The control concept introduced here is thus akin to the problem of photon assisted transfer, a theory of which in nanojunctions with metallic contacts was developed and applied in Refs. [3,22]. In these works a time dependent level shift in a molecule bridging two metal electrodes arises from the coupling to an oscillating dipole field (see below). For a single site bridge this coupling may be described by a permanent dipole moment [8]. The above qualitative discussion is quantified in the next section.

3. Theory

In this section we develop and discuss our theoretical framework. We begin in Section 3.1 with a description of the model Hamiltonian and proceed (Section 3.2) with the density matrix formulation. Sections 4 and 5 specialize our theory to the cases of a single- and a double-site molecular bridge.

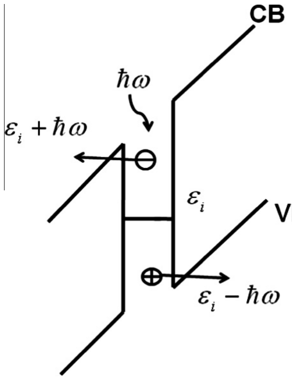

Figure 1. Electromagnetic excitation applied to a molecular bridge in state ε_i leads to generation of its photonic replica at energies $\varepsilon_i \pm \hbar\omega$. Tunnelling from the photonic replica results in a unidirectional photocurrent. CB, conduction band; VB, valence band.

3.1. Model

The complete Hamiltonian describing a molecular bridge interacting with two semiconductor electrodes and subject to a low frequency optical pulse is written as,

$$\hat{H} = \hat{H}^0_{wire} + \hat{H}_{SC} + \hat{\Delta} + \hat{W} + \hat{V} \tag{1}$$

where the zero order wire Hamiltonian,

$$\hat{H}^0_{wire} = \sum_{n=1}^{N} \varepsilon_n \hat{c}_n^\dagger \hat{c}_n \tag{2}$$

is described as a tight-binding model composed of N sites, where each site represents available orbitals (e.g., the HOMO and/or the LUMO), ε_n denotes the electron energy on site n and $\hat{c}_n^\dagger$ ($\hat{c}_n$) are creation (annihilation) operators for electrons in site n. The Hamiltonian of the intrinsic semiconductor leads is given as,

$$\hat{H}_{SC} = \sum_{n=1,N} \sum_{k\in K_n} (\varepsilon_{ck}\hat{c}^\dagger_{ck}\hat{c}_{ck} + \varepsilon_{vk}\hat{c}^\dagger_{vk}\hat{c}_{vk}) \tag{3}$$

where c (v) denote the conduction (valence) bands and $\varepsilon_{c(v)k}$ are the corresponding quasicontinuum electron energies. In what follows we will omit the band indices c and v when not essential, so as to simplify the notation. We denote by K_1 the lead in contact with bridge site $n = 1$ and by K_N the lead in contact with site $n = N$. The operator $\hat{\Delta}$ in Eq. (1) accounts for electron transfer interactions between nearest sites within the Huckel model,

$$\hat{\Delta} = -\sum_{n=1}^{N-1} \Delta(\hat{c}^\dagger_{n+1}\hat{c}_n + \hat{c}^\dagger_n\hat{c}_{n+1}), \tag{4}$$

and $\hat{W}(t) = -\mathbf{D}\cdot\mathbf{E}(t)$ describes the interaction of the bridge sites with an external electromagnetic field $\mathbf{E}(t)$, where the dipole operator has only diagonal elements,

$$D_{mm} = D[\delta_{N1} + (N + 1 - 2m)/2]. \tag{5}$$

Here D is given by the product of electron charge by the distance between the neighboring sites [3,22], and δ_{N1} is the Kronecker delta. Finally,

$$\hat{V} = \sum_{n=1,N;k\in K_n} (V_{nck}\hat{c}^{\dagger}_{ck}\hat{c}_n + V_{n\upsilon k}\hat{c}^{\dagger}_{\upsilon k}\hat{c}_n) + h.c., \tag{6}$$

where *h.c.* denotes Hermitian conjugate. Eq. (6) describes electron transfer between the molecular bridge and the leads, thus giving rise to net current via the biased junction.

We consider electronic transport through the molecular wire, where the semiconductor leads $K_n, n = 1, N$ are taken to be each in its own equilibrium characterized by its temperature T (here taken equal for the two leads) and electronic electrochemical potentials $\mu_{K_n c}$ and $\mu_{K_n \upsilon}$ for the conduction and valence bands, respectively. Therefore, the lead electrons are described by the equilibrium Fermi functions

$$f_{K_n}(\varepsilon_{c(\upsilon)k}) = [exp((\varepsilon_{c(\upsilon)k} - \mu_{K_n c(\upsilon)})\Big/k_BT) + 1]^{-1}, \tag{7}$$

where k_B is Boltzmann's constant. Consequently, the expectation values for the lead operators are simplified through the relation $\langle \hat{c}^{\dagger}_{c(\upsilon)k}\hat{c}_{c(\upsilon)k'}\rangle = f_{K_n}(\varepsilon_{c(\upsilon)k})\delta_{kk'}$.

3.2. Equations of motion

Our analysis is based on the generalized master equation for the reduced density matrix of the molecular subsystem treating $\hat{V}$ as a perturbation [3,23,24]. Briefly, one starts with the equation of motion for the total density operator

$$\frac{d\hat{\rho}}{dt} = -\frac{i}{\hbar}[\hat{H}_0 + \hat{V}, \hat{\rho}], \tag{8}$$

where

$$\hat{H}_0 = \hat{H}_{SC} + \hat{H}^0_{\text{wire}} + \hat{\Delta} + \hat{W} \tag{9}$$

and the interactions constituting $\hat{H}_0$ are defined in the previous subsection. Transforming to the interaction representation through the unitary transformation,

$$\hat{B}^{int} \to \hat{S}^{-1}\hat{B}\hat{S}, \tag{10}$$

where the unitary operator $\hat{S}$ satisfies the equations

$$i\hbar\frac{d\hat{S}}{dt} = \hat{H}_0\hat{S}, \hat{S}^{\pm 1}(t = 0) = I, \tag{11}$$

we derive an evolution equation for the reduced density matrix describing the discrete manifold by introducing projectors onto the left (L) and right (R) quasicontinua, defined through, $P_K\rho(t) = \rho_K \text{Tr}_K\rho(t), K = L, R$. As illustrated in Ref. [25], the resulting equation of motion satisfied by the reduced density matrix $\sigma(t) = \text{Tr}_R\text{Tr}_L\rho(t)$ is given to second order with respect to $\hat{V}$ as,

$$\frac{d\sigma^{int}(t)}{dt} = -\frac{1}{\hbar^2}\text{Tr}_{L,R}\int_0^t d\tau[\hat{V}^{int}(t), [\hat{V}^{int}(t-\tau), \sigma^{int}(t-\tau)\rho_K]] \tag{12}$$

where $\text{Tr}_{L,R} = \text{Tr}_L\text{Tr}_R$. Reexpressing the coupling Hamiltonians $\hat{V}$ (Eq. (6)) as

$$\hat{V} = \sum_{n=1,N}(\hat{c}_n\Lambda^{\dagger}_n + \hat{c}^{\dagger}_n\Lambda_n) \tag{13}$$

where $\Lambda_n = \sum_{k\in K_n} V_{nk}\hat{c}_k$, we have $\hat{V}^{int}(t) = \hat{c}^{+int}_n(t)\Lambda^{int}_n(t) + \hat{c}^{int}_n(t)\Lambda^{\dagger int}_n(t)$ with $\Lambda^{int}_n(t) = \sum_{k\in K_n} V_{nk}\hat{c}_k \exp(-\frac{i}{\hbar}\varepsilon_k t)$.

With Eq. (13), the RHS of Eq. (12) can be expressed in terms of reservoir correlation functions that reflect the reservoir equilibrium properties as well as the nature of its interaction with the wire. For example,

$$\text{Tr}_{L,R}[\Lambda^{int}_n(t)\Lambda^{\dagger int}_n(t-\tau)\rho_K] = \sum_{k\in K_n}|V_{kn}|^2[1 - f_{K_n}(\varepsilon_k)]\exp(-\frac{i}{\hbar}\varepsilon_k\tau) \tag{14}$$

As a result, we get from Eq. (12)

$$\begin{aligned}\frac{d\sigma^{int}(t)}{dt} = \frac{1}{\hbar^2}\sum_{nk\in K_n}|V_{kn}|^2\int_0^t d\tau\{-\{&\hat{c}^{int}_n(t)\hat{c}^{+int}_n(t-\tau)f_{K_n}(\varepsilon_k)\exp(i\omega_k\tau)\\ &+\hat{c}^{+int}_n(t)\hat{c}^{int}_n(t-\tau)[1 - f_{K_n}(\varepsilon_k)] \times \exp(-i\omega_k\tau)\}\sigma^{int}(t-\tau)\\ &+\hat{c}^{int}_n(t)\sigma^{int}(t-\tau)\hat{c}^{+int}_n(t-\tau)[1 - f_{K_n}(\varepsilon_k)]\exp(i\omega_k\tau)\\ &+\hat{c}^{+int}_n(t)\sigma^{int}(t-\tau)\hat{c}^{int}_n(t-\tau)f_{K_n}(\varepsilon_k)\exp(-i\omega_k\tau)\\ &+\hat{c}^{+int}_n(t-\tau)\sigma^{int}(t-\tau)\hat{c}^{int}_n(t)f_{K_n}(\varepsilon_k)\exp(i\omega_k\tau)\\ &+\hat{c}^{int}_n(t-\tau)\sigma^{int}(t-\tau)\hat{c}^{+int}_n(t)[1 - f_{K_n}(\varepsilon_k)]\exp(-i\omega_k\tau)\\ &-\sigma^{int}(t-\tau)\{\hat{c}^{int}_n(t-\tau)\hat{c}^{+int}_n(t)f_{K_n}(\varepsilon_k)\exp(-i\omega_k\tau)\\ &+\hat{c}^{+int}_n(t-\tau)\hat{c}^{int}_n(t)[1 - f_{K_n}(\varepsilon_k)]\exp(i\omega_k\tau)\}\},\end{aligned} \tag{15}$$

where $\omega_k = \varepsilon_k/\hbar$.

Eq. (15) is clearly non-Markovian, memory effects being introduced via the dependence of the σ^{int} on the RHS on τ. We proceed by expanding the interaction picture creation and annihilation operators ($\hat{c}^{\dagger int}_n(t)$ and $\hat{c}^{int}_n(t)$, respectively) contained in $\hat{V}^{int}(t)$, in a Fourier series as [20],

$$\hat{c}^{\dagger int}_n(t) = \sum_r \hat{c}^{\dagger r}_n exp(i\omega_r t) \text{ and } \hat{c}^{int}_n(t) = \sum_q \hat{c}^q_n exp(-i\omega_q t) \tag{16}$$

and invoking the Markovian approximation by neglecting the τ-dependence of $\sigma^{int}(t-\tau)$ in Eq. (15). Taking the $t \to \infty$ limit for the upper limit of integration with respect to τ, we can then approximate Eq. (15) as,

$$\begin{aligned}&\frac{d\sigma^{int}(t)}{dt} + i\sum_{nrq}[\delta^{rq}_n\hat{c}^{+r}_n\hat{c}^q_n, \sigma^{int}(t)]_-\\ &\quad = \sum_{nrq}\gamma^{rq}_n\{-[([\hat{c}^q_n, \hat{c}^{+r}_n]_- f_{K_n}(\hbar\omega_r) + \hat{c}^{+r}_n\hat{c}^q_n), \sigma^{int}(t)]_+\\ &\qquad + 2\hat{c}^q_n\sigma^{int}(t)\hat{c}^{+r}_n[1 - f_{K_n}(\hbar\omega_r)] + 2\hat{c}^{+r}_n\sigma^{int}(t)\hat{c}^q_n f_{K_n}(\hbar\omega_r)\},\end{aligned} \tag{17}$$

where $[\hat{A}, \hat{B}]_-$ denotes the commutator of $\hat{A}$ and $\hat{B}$, and $[\hat{A}, \hat{B}]_+$ their anticommutator, $[\hat{A}, \hat{B}]_\pm = \hat{A}\hat{B} \pm \hat{B}\hat{A}$,

$$\delta^{rq}_n = -\frac{1}{\hbar^2}\sum_k |V_{kn}|^2\exp[i(\omega_r - \omega_q)t]\xi(\omega_r - \omega_q)\frac{P}{\omega_k - \omega_r} \tag{18}$$

P denotes the principal value, and

$$\gamma^{rq}_n = \frac{\pi}{\hbar^2}\sum_k |V_{kn}|^2\exp[i(\omega_r - \omega_q)t]\xi(\omega_r - \omega_q)\delta(\omega_k - \omega_r) \tag{19}$$

is the spectral function. The Fourier components index $r(q)$ in Eqs. (16)–(19) will be seen shortly to have the physical significance of the photonic replication of order $r(q)$. The spectral functions of Eq. (19) with $r = q$ will thus take the role of r-specific decay rates due to coupling of the r^{th} dressed state with the K_n quasi-continuum. The frequency dependence of γ^{rr}_n may be neglected provided that γ^{rr}_n is small relative to the bath correlation frequency ω_c – the range over which its spectral density essentially changes. In Eqs. (18) and (19) we retained only the terms giving the dominant contributions, for which $|\omega_r - \omega_q| \ll \omega_c$. This was done by introducing a switching function $\xi(\omega_r - \omega_q)$ defined as $\xi(\omega_r - \omega_q) = 0$ for $|\omega_r - \omega_q| \gtrsim \omega_c$, and $\xi(\omega_r - \omega_q) = 1$ for $|\omega_r - \omega_q| \ll \omega_c$. In the latter case γ^{rq}_n might depend on time $\sim \exp[i(\omega_r - \omega_q)t]$ if $\omega_r \neq \omega_q$.

A back transformation to the Schrodinger representation via the unitary transformation

$$\hat{B} \to \hat{S}\hat{B}^{int}\hat{S}^{-1}, \tag{20}$$

yields

$$\frac{d\sigma}{dt}+\frac{i}{\hbar}\left[\hat{H}_0+\hbar\sum_{nrq}\delta_n^{rq}\hat{C}_n^{\dagger r}\hat{C}_n^q,\sigma\right]_-=\sum_{nrq}\gamma_n^{rq}\{-[([\hat{C}_n^q,\hat{C}_n^{\dagger r}]_-f_{K_n}(\hbar\omega_r)+\hat{C}_n^{\dagger r}\hat{C}_n^q),\sigma]_++2\hat{C}_n^q\sigma\hat{C}_n^{\dagger r}+2(\hat{C}_n^{\dagger r}\sigma\hat{C}_n^q-\hat{C}_n^q\sigma\hat{C}_n^{\dagger r})f_{K_n}(\hbar\omega_r)\}, \tag{21}$$

where,

$$\hat{C}_n^q=\hat{S}\hat{c}_n^q\hat{S}^{-1},\hat{C}_n^{\dagger r}=\hat{S}\hat{c}_n^{+r}\hat{S}^{-1}. \tag{22}$$

Eq. (21) will be used below to calculate the reduced density matrix of the molecular bridge and the corresponding currents.

4. Single site molecular bridge

In this section we specialize the theory developed in the previous section to the simplest case scenario of a single site bridge. This simple case has the advantageous feature of allowing analytical expressions for the time evolution of the reduced density matrix and for the electron and hole currents, which are shown below to provide useful insights. The analytical theory is presented in Section 4.2 for the symmetric case depicted in Figure 1, where the molecular energy level ε_i is energetically close to the center of the band gap and the dressed energies $\varepsilon_i+\hbar\omega$ and $\varepsilon_i-\hbar\omega$ are close to the conduction and valence bands, respectively. In Section 4.4 we generalize the discussion to the case of an asymmetric junction, where, in the extreme case, only a single photonic replication (with energy $\varepsilon_i+\hbar\omega$ or $\varepsilon_i-\hbar\omega$) contributes to the current, and illustrate that the conclusions derived for the symmetric case are not modified. In Section 4.3 we illustrate a new and fundamentally interesting phenomenon, namely zeros of the light-induced currents as a function of the interaction strength, which are reminiscent of the phenomenon of coherent destruction of tunneling [3,8,26–30], and which we term coherent destruction of induced tunneling.

Solving Eqs. (11) in the limit of a single site bridge, one finds for the S-matrix elements

$$S_{ii}=(S_{ii}^{-1})^*=\exp[-i\omega_i t+iz_i\sin(\omega t)] \tag{23}$$

where $\omega_i=\varepsilon_i/\hbar$, $z_i=\mathbf{D}_{ii}\cdot\mathbf{E}_0/(\hbar\omega)$. The right-hand side of Eq. (23) can be expanded in terms of the Bessel functions $J_s(z_i)$ as [31]

$$\exp[-i\omega_i t+iz_i\sin(\omega t)]=\sum_{s=-\infty}^{s=\infty}J_s(z_i)\exp[i(s\omega-\omega_i)t] \tag{24}$$

This expansion is readily extended to the case of excitation of the molecular bridge by pulsed, rather than continuous wave (CW) light, $E(t)=E_0(t)\cos\omega t$ (whose pulse duration is long with respect to the optical cycle [21]). In that case the interaction parameter, $z_i(t)=\mathbf{D}_{ii}\cdot\mathbf{E}_0(t)/(\hbar\omega)$, acquires a time-dependence.

Using the equation of motion (21), one obtains relations for the expectation values of the molecular bridge operators

$$P_{i'i}=\langle\hat{c}_i^\dagger\hat{c}_{i'}\rangle\equiv\mathrm{Tr}(\hat{c}_i^\dagger\hat{c}_{i'}\sigma)=P_{ii'}^* \tag{25}$$

that are binary in the creation and annihilation operators for electrons in the molecular states. The time evolution of the molecular bridge population P_{ii} obtained with Eqs. (21)–(24), reduces under the conditions of Figure 1 to,

$$\frac{dP_{ii}}{dt}=\sum_n[2(1-P_{ii})\Gamma_{vK_n,i}-2P_{ii}\Gamma_{cK_n,i}] \tag{26}$$

where

$$\Gamma_{vK_n,i}=\sum_{r=1}^{\infty}J_r^2(z_i)\gamma_{vK_n,i}^{rr},\Gamma_{cK_n,i}=\sum_{r=-\infty}^{-1}J_r^2(z_i)\gamma_{cK_n,i}^{rr}, \tag{27}$$

and

$$\gamma_{c,vK_n,i}^{rr}=\frac{\pi}{\hbar^2}\sum_k|V_{c,vki}|^2\delta(\omega_k-\omega_i+r\omega) \tag{28}$$

are the spectral functions of Eq. (19), which take the significance of replication-specific decay rates due to coupling of the bridge site with the conduction (c) and the valence (v) band of the electrode. For the specific model depicted in Figure 1, $\gamma_{vL,i}^{11}=\gamma_{cR,i}^{-1,-1}=0$, and, given that only a single site is included ($N=1$), we replaced the $K_n,n=1,N$ notation by $K_1=L$ for the left electrode and $K_N=R$ for the right electrode of the single site junction.

Eq. (27) describes the rate of electron transfer between the molecular state i and the conduction (valence) bands ($\Gamma_{c(v)L(R),i}$) as a sum over contributions of electron transfer rates $\gamma_{c(v)R(L),i}^{rr}$, in which the underlying potential coupling constants $V_{c(v)ki}$ are evaluated in the absence of the laser field but the energy-conserving δ-function tunes the electron energy to the r-photonic replication, that is, to the side-band energy $\hbar\omega_i\pm|r|\hbar\omega$ shifted by integer multiples of the photon quantum. The dependence on the interaction strength, $z_i=\mathbf{D}_{ii}\cdot\mathbf{E}_0/(\hbar\omega)$, is solely contained in the squared Bessel functions in Eq. (27), which serve as weight functions for the $\gamma_{c(v)R(L),i}^{rr}$ components of $\Gamma_{c(v)L(R),i}$. Note that the partial electron transfer rates $J_r^2(z_i)\gamma_{cL(R),i}^{rr}$ and $J_r^2(z_i)\gamma_{vL(R),i}^{rr}$ contain contributions from negative and positive r-values, respectively. Thus, the photon absorption ($r<0$) and emission ($r>0$) processes can be viewed as creating effective molecular states at energies $\hbar\omega_i+r\hbar\omega$ with probabilities $J_r^2(z_i)$. These probabilities decay rapidly with r when $|z_i|<1$.

In the pulsed regime, the Markovian Eq. (26) is valid for pulses longer than reciprocal correlation frequency $1/\omega_c$. For shorter pulses the non-Markovian Eq. (12) has to be used.

4.1. Unidirectional currents and transferred charge

The electronic current $I_{L,R}$ is given by the rate at which the number of electrons changes in lead L,R [4,24,32]

$$I_K=e\frac{d}{dt}\sum_{k\in L(R)}\langle\hat{n}_k\rangle=\frac{ie}{\hbar}\sum_{k\in L(R)}\langle[\hat{H},\hat{n}_k]\rangle=\frac{ie}{\hbar}\sum_{k\in L(R)}\mathrm{Tr}([\hat{H}_0+\hat{V},\hat{n}_k]\hat{\rho}), \tag{29}$$

where $\hat{n}_k=\sum_{p=c,v}\hat{c}_{pk}^\dagger\hat{c}_{pk}$. Evaluating the commutator in Eq. (29), we find,

$$I_{L(R)}=\frac{ie}{\hbar}\sum_{k\in L(R)}\langle[\hat{H},\hat{n}_k]\rangle=\frac{2e}{\hbar}\sum_{k\in L(R)}\sum_{p=c,v}\mathrm{Im}(V_{ipk}\langle\hat{c}_{pk}^\dagger\hat{c}_i\rangle). \tag{30}$$

Using the Heisenberg equations of motion, one obtains an equation of motion for the expectation value of operator $\hat{c}_{pk}^\dagger\hat{c}_i$ (see also Eq. (12) of Ref. [4]) reading,

$$\frac{d}{dt}\langle\hat{c}_{pk}^\dagger\hat{c}_i\rangle=i\left[\omega_k-(\omega_i+\frac{1}{\hbar}W_{ii})\right]\langle\hat{c}_{pk}^\dagger\hat{c}_i\rangle+\frac{i}{\hbar}V_{ipk}^*[P_{ii}-f_{L(R)}(\varepsilon_k)], \tag{31}$$

where $k\in L(R), W_{ii}$ is the matrix element of the interaction of the bridge site with the external electromagnetic field (see below Eq. (4)). Formally integrating the last equation, using expansion (24), invoking the Markovian approximation, and substituting the result into the right-hand side of Eq. (30), we obtain

$$I_K=-2e[(1-P_{ii})\Gamma_{vK,i}-P_{ii}\Gamma_{cK,i}]. \tag{32}$$

An observable quantity in pulsed experiments is the charge transferred during an electromagnetic pulse, $Q_{L(R)}=\int_0^\infty I_{L(R)}(t)dt$. Using Eq. (32), Eq. (26) can be written as

$$\frac{dP_{ii}}{dt}=-I_R/e-I_L/e \tag{33}$$

The right-hand side of Eq. (26) is proportional to the sum of the currents, $I_R(t)$ and $I_L(t)$, due to the coupling of state i with the right and left electrodes, respectively.

Integrating Eq. (33) from $t = 0$ to $t = \infty$, we get,

$$e[P_{ii}(\infty) - P_{ii}(0)] = -Q_R - Q_L \tag{34}$$

Eq. (34) expresses the charge conservation – the transferred charges value $-Q_R$ and Q_L coincide only for $P_{ii}(\infty) = P_{ii}(0)$. This is achieved when the pulse is long with respect to the tunneling lifetime (see below). It is readily seen that current in the SC-molecule-SC junction exists only in the presence of external EM field ($z \neq 0$) – in the absence of the laser pulse both I_R and I_L vanish.

4.2. An analytically soluble model

The first order differential Eq. (26) can be readily integrated, giving, for $P_{ii}(0) = 0$ and excitation by a rectangular pulse of duration t_p,

$$\begin{aligned} I_{K_n} = \frac{2e}{\Gamma_{vi}+\Gamma_{ci}}\{(&\Gamma_{cK_n,i}\Gamma_{vK_{n'},i} - \Gamma_{vK_n,i}\Gamma_{cK_{n'},i}) \\ &- (\Gamma_{cK_n,i}+\Gamma_{vK_n,i})\Gamma_{vi}\exp[-2(\Gamma_{vi}+\Gamma_{ci})t]\} \end{aligned} \tag{35}$$

where $n \neq n'$, $\Gamma_{vi} = \sum_{K_n}\Gamma_{vK_n,i}$ and $\Gamma_{ci} = \sum_{K_n}\Gamma_{cK_n,i}$ are the rates of electron transfer between the molecular state i and the valence and conduction bands, respectively, of the two leads, and we used Eq. (32). In the steady-state limit, Eq. (35) reduces to,

$$I_L = 2e\frac{\Gamma_{cL,i}\Gamma_{vR,i} - \Gamma_{vL,i}\Gamma_{cR,i}}{\Gamma_{vi}+\Gamma_{ci}} = -I_R, \tag{36}$$

i.e., as expected, under steady state conditions the currents are equal.

In the weak field limit, where the field-matter interaction parameter is small with respect to unity, $|z_i| \ll 1$, we obtain from Eq. (35)

$$I_R(t) = \frac{-2e\Gamma_R}{\Gamma_R+\Gamma_L}\{\Gamma_L + \Gamma_R\exp[-2(\Gamma_R+\Gamma_L)t]\}, \tag{37}$$

and

$$I_L(t) = \frac{2e\Gamma_L\Gamma_R}{\Gamma_R+\Gamma_L}\{1 - \exp[-2(\Gamma_R+\Gamma_L)t]\}, \tag{38}$$

where the dependence on the bias voltage and the laser parameters is implicit in the $\Gamma_R = J_1^2(z_i)\gamma^{11}_{vR,i}$ and $\Gamma_L = J_1^2(z_i)\gamma^{-1,-1}_{cL,i}$. Eqs. (37) and (38) illustrate that the hole current, $-I_R$, starts out at a finite value, $2e\Gamma_R$, and decays exponentially according to the tunneling lifetime $[2(\Gamma_L+\Gamma_R)]^{-1}$, which serves as a natural system time-scale, building up negative charge on the bridge. The electron current, I_L, starts at zero and grows at the same rate, the tunneling rate, as negative charge builds up on the bridge. This behavior is summarized in Figure 2, where $-I_R(t)$ and $I_L(t)$ are plotted versus time along with $dP_{ii}/dt = -I_R/e - I_L/e$, Eq. (33).

In the steady-state regime both currents converge to,

$$I_L = -I_R = 2e\frac{\Gamma_L\Gamma_R}{\Gamma_L+\Gamma_R}, \tag{39}$$

a specific case of Eq. (36) for $|z_i| \ll 1$. Eq. (39) asserts that at steady state the rates of negative charge transported onto and out of the bridge via the valence and conduction bands, respectively, are equal.

At short time $dP_{ii}/dt = -I_R/e - I_L/e$, Eq. (33), is positive (see Figure 2), i.e., the charge density on the bride grows at a constant rate determined by Γ_R. As electron current develops, the rate of change of P_{ii} drops, until it stabilizes on zero at steady state, where the charge density on the bridge remains constant. For pulses short with respect to the tunneling time, however, steady state is never established and P_{ii} maintains its time dependence throughout.

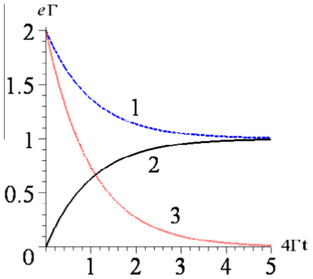

Figure 2. The hole and electron currents, $-I_R(t)$ (1) and $I_L(t)$ (2), respectively, and the rate $dP_{ii}/dt = -I_R(t) - I_L(t)$ (3) of Eq. (33) versus time for $\Gamma_R = \Gamma_L \equiv \Gamma$ and $|z_i| \ll 1$.

According to the charge conservation relation, Eq. (34), the transferred charges $-Q_R$ and Q_L coincide only for $P_{ii}(\infty) = P_{ii}(0)$ when the pulse is long with respect to the tunneling lifetime, $t_p \gg [2(\Gamma_L+\Gamma_R)]^{-1}$. Eqs. (37), (38) illustrate also the possibility of generating unidirectional current at times short with respect to $[2(\Gamma_L+\Gamma_R)]^{-1}$.

To develop general insight into the magnitude of the electric field that would be needed to generate significant currents, we consider a pulsed laser experiment as described in Ref. [17], where one observes the time-integrated current, $I_{int} = Qf$, equal to the product of the charge transferred during an electromagnetic pulse, $Q\,(\simeq e\Gamma t_p)$, and the laser pulse repetition frequency, $f\,(\simeq 100$ MHz). A measurable value of the time-integrated current is about $I_{int} \sim 1 - 10pA$[17]. In such a situation, we evaluate the necessary field strength of the laser pulse to be $\sim 10^6 V/cm$ for $|z_i| = 0.3, \gamma^{11}_{vR,i} = \gamma^{-1,-1}_{cL,i} = 10ps^{-1}$, and $t_p = 1ps$ [17].

4.3. Coherent destruction of induced tunneling (CDIT)

We proceed to consider the steady-state current, Eq. (36), when the interaction parameter $|z_i|$is not small with respect to unity. For broad conduction and valence bands and $|r| > 1$, it may be expected that, due to symmetry, the spectral functions of the r-th order replication would be equal for the left and right contacts, i.e.,

$$\gamma^{rr}_{cL,i} = \gamma^{rr}_{cR,i} \text{ and } \gamma^{rr}_{vR,i} = \gamma^{rr}_{vL,i} \tag{40}$$

In this case Eq. (36) takes the form

$$I_L = -I_R = 2eJ_1^2(z_i)\frac{\gamma^{-1,-1}_{cL,i}(\Gamma_{vR,i} - \gamma^{11}_{vR,i}) + \gamma^{11}_{vR,i}\Gamma_{cL,i}}{\Gamma_{vi}+\Gamma_{ci}}. \tag{41}$$

Eq. (41) shows that the steady-state current is proportional to the square of the first-order Bessel function $J_1^2(z_i)$. This implies that the current vanishes identically at zeros of $J_1(z_i)$ (i.e., for $z_i = 0, 3.8, 7, \ldots$). The phenomenon observed in Eq. (41) is referred to in what follows as coherent destruction of induced tunneling (CDIT), as it extends the extensively studied problem of coherent destruction of tunneling (CDT), related to zeros of $J_0(z_i)$[3,8,26–30] to the case of light-induced tunneling. In the present case the effect could be formulated as dressing of the laser-free coupling of the molecular bridge with semiconductor leads, $V_{c(v)ki}$, by the light field to make the effective coupling,

$$V_{c(v)ki} \to (V_{c(v)ki})_{eff} = J_{\mp 1}(z_i)V_{c(v)ki}$$

for the electron transfer rates $\gamma^{-1,-1}_{cL,i}$ and $\gamma^{11}_{vR,i}$ (see Eq. (41)). These effective tunneling matrix elements $(V_{c(v)ki})_{eff}$ are suppressed at zeros of $J_{\mp 1}(z_i)$.

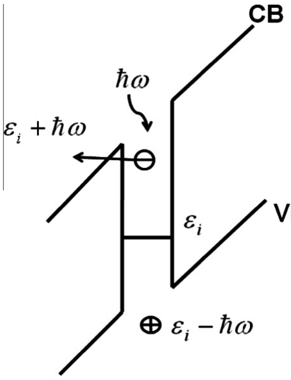

Figure 3. Photonic replica for an asymmetric location of the molecular energy level. Tunnelling from the upper photonic replication at $\varepsilon_i + \hbar\omega$ results in a unidirectional photocurrent.

4.4. Asymmetric location of the molecular energy level

In this subsection we briefly generalize the discussion of the previous subsections to the case where the energetic location of the molecular orbital i is asymmetric with respect to the conductance and valence bands of the SC leads. We illustrate that the results obtained via consideration of the idealized symmetric case remain valid. For concreteness, we assume that the higher first photonic replication is coupled only with the conductance band of the left lead whereas the lower first photonic replication is coupled with the valence bands of both leads, Figure 3.

In this case, steady-state current is determined by the same expressions, Eqs. (36) and (40), the sole difference being that now $\gamma_{vL,i}^{11} \neq 0$ and we assume that $\gamma_{vR,i}^{11} = \gamma_{vL,i}^{11}$, which is realized, as discussed above, for broad valence and conduction bands. In this case Eq. (36) takes the form,

$$I_L = -I_R = 2eJ_1^2(z_i)\frac{\gamma_{cL,i}^{-1,-1}\Gamma_{vR,i}}{\Gamma_{vi} + \Gamma_{ci}}, \tag{42}$$

which gives for $|z_i| \ll 1$,

$$I_L = -I_R = 2e\frac{\Gamma_L\Gamma_R}{2\Gamma_R + \Gamma_L} \tag{43}$$

since $\gamma_{vR,i}^{11} = \gamma_{vL,i}^{11}$ and $\Gamma_R = J_1^2(z_i)\gamma_{vR,i}^{11}$.

Eqs. (42) and (43) show that the photoinduced, unidirectional current survives for an asymmetric position of a molecular orbital with respect to the conduction and valence bands of the SC leads, thus illustrating the robustness of the proposed method. The value of the current, however, is somewhat smaller than that in the symmetric case (see Eqs. (39) and (41)). Eq. (42) shows also that the effect of CDIT likewise persists in the asymmetric case.

5. A two-site molecular bridge

In this section we consider the case of a two-site molecular bridge in contact with SC leads. Specifically, we envision two molecular sites of energies ε_1 and ε_2 (Figure 4) that are excited by EM field $\mathbf{E}(t) = \mathbf{E}_0\cos(\omega t)$ tuned to a sub-bandgap frequency ω, such that the dressed energies $\varepsilon_{1,2} + \hbar\omega$ and $\varepsilon_{1,2} - \hbar\omega$ are close to the conduction and valence bands, respectively. The sites are coupled to each other due to the intersite interaction Δ of Eq. (4), and interact with the EM field due to site permanent dipole moments $\mathbf{D}_{11} = -\mathbf{D}_{22} \equiv \mathbf{D}/2$, Eq. (5), [3,8,28,30].
In the limit of a small energy gap $|E_2 - E_1|/\hbar$ and weak coupling $\Delta/\hbar$,

$$\hbar\omega \gg |\Delta|, |E_2 - E_1|, \tag{44}$$

the operator $\hat{S}$, Eq. (11), can be conveniently represented as a product of two operators

$$\hat{S} = \hat{S}'\hat{S}'' \tag{45}$$

where $\hat{S}'$ and $\hat{S}''$ obey the equations [19]

$$i\hbar\frac{d\hat{S}'}{dt} = (\hat{H}_{wire}^0 + W)\hat{S}', \tag{46}$$

$$i\hbar\frac{d\hat{S}''}{dt} = (\hat{S}'^{-1}\hat{\Delta}\hat{S}')\hat{S}''. \tag{47}$$

Eq. (45) partitions the trasformation operator $\hat{S}$ into a fast and a slow component, $\hat{S}'$ and $\hat{S}''$, respectively, where the quasi-static evolution of the slow component follows from the condition (44). The time evolution of the rapid component, Eq. (46), is given by Eq. (23) above. Assuming that $|\Delta|$ and $|E_2 - E_1|$ are smaller than the bath correlation frequency ω_c, the characteristic time of change of the slow component, $\hat{S}''$, is larger than the bath correlation time ω_c^{-1}, and its time-dependence does not influence the relaxation parameters. Under these assumptions one can thus replace the expansion of the interaction picture operators $\hat{c}_n^{+int}(t) = \hat{S}''^{-1}(t)\hat{S}'^{-1}(t)\hat{c}_n^{+}\hat{S}'(t)\hat{S}''(t)$ and $\hat{c}_n^{int}(t) = \hat{S}''^{-1}(t)\hat{S}'^{-1}(t)\hat{c}_n\hat{S}'(t)\hat{S}''(t)$ in a Fourier series, Eq. (16), by the simplified expansion,

$$\begin{aligned}
\hat{S}'^{-1}(t)\hat{c}_n^{+}\hat{S}'(t) &= \sum_r \hat{c}_n'^{+r}\exp(i\omega_r t) \\
&= \hat{c}_n^{\dagger}\sum_{r=-\infty}^{\infty} J_r(z_n)\exp[i(\omega_n - r\omega)t], \\
\hat{S}'^{-1}(t)\hat{c}_n\hat{S}'(t) &= \sum_q \hat{c}_n'^{q}\exp(-i\omega_q t) \\
&= \hat{c}_n\sum_{q=-\infty}^{\infty} J_q(z_n)\exp[-i(\omega_n - q\omega)t]
\end{aligned} \tag{48}$$

defined in terms of only the rapidly changing operator $\hat{S}'(t)$. As above, site n is coupled with electrode K_n. In writing Eqs. (48) we used Eqs. (23) and (24). Substituting expansions (48) into Eq. (15), invoking the Markovian approximation, and transforming back to the Schrodinger representation via the unitary transformation, Eq. (20), we finally obtain,

$$\begin{aligned}
&\frac{d\sigma}{dt} + \frac{i}{\hbar}\left[\hat{H}_0 + \hbar\sum_{nr} J_r^2(z_n)\delta_n^{rr}\hat{c}_n^{\dagger}\hat{c}_n, \sigma\right] \\
&\quad = -\sum_{nr} J_r^2(z_n)\gamma_n^{rr}\{2f_{K_n}[\hbar(\omega_n - r\omega)]\sigma + [\hat{c}_n^{\dagger}\hat{c}_n\sigma + \sigma\hat{c}_n^{\dagger}\hat{c}_n](1 \\
&\qquad - 2f_{K_n}[\hbar(\omega_n - r\omega)]) - 2\hat{c}_n\sigma\hat{c}_n^{\dagger}[1 - f_{K_n}(\hbar(\omega_n - r\omega))] \\
&\qquad - 2\hat{c}_n^{\dagger}\sigma\hat{c}_n f_{K_n}(\hbar(\omega_n - r\omega))\}.
\end{aligned} \tag{49}$$

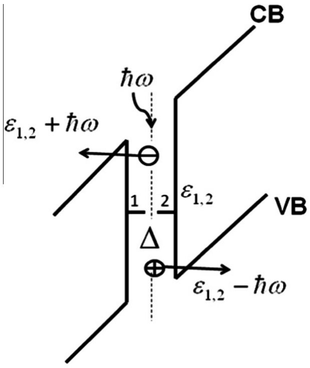

Figure 4. Two-site molecular bridge. The sites are coupled to each other due to intersite interaction Δ, and posses permanent dipole moments $\mathbf{D}_{11} = -\mathbf{D}_{22} \equiv \mathbf{D}/2$.

With the time evolution of $\sigma(t)$ determined, we return to the expectation values of the molecular bridge operators, Eq. (25), obtaining under the conditions of Figure 4 equations of motion for the polarization P_{12} and the populations $P_{nn}, n = 1, 2$ that, in turn, determine the light-induced hole and the electron currents in the two-site junction. In particular,

$$\frac{dP_{12}}{dt}+i\left(\bar{\omega}_{12}-\frac{\mathbf{D}\cdot\mathbf{E}}{\hbar}\right)P_{12}+\frac{i}{\hbar}\Delta(P_{11}-P_{22}) = -P_{12}(\Gamma_{vL,1}+\Gamma_{cL,1}+\Gamma_{vL,2}+\Gamma_{cL,2}) \qquad (50)$$

where

$$\bar{\omega}_{12}=\frac{1}{\hbar}\left[(E_1-E_2)+\hbar\sum_r J_r^2(z_1)(\delta_1^{rr}-\delta_2^{rr})\right] \qquad (51)$$

and

$$\frac{dP_{nn}}{dt}+\frac{2}{\hbar}(-1)^n\Delta\mathrm{Im}P_{12}=2\Gamma_{vK_n,n}(1-P_{nn})-2\Gamma_{cK_n,n}P_{nn} \qquad (52)$$

Similar to Ref. [23], we define the electronic current I for two-sites case as the rate of change of electron population on the left of the dashed line in Figure 4,

$$I=\frac{ie}{\hbar}\Delta(P_{21}-P_{12})=\frac{2e}{\hbar}\Delta\mathrm{Im}P_{12}. \qquad (53)$$

Introducing the transformation

$$P_{12}=\tilde{P}_{12}\exp\{-i[\bar{\omega}_{12}t-\frac{1}{\hbar}\int_0^t\mathbf{D}\cdot\mathbf{E}(t')dt']\}, \qquad (54)$$

one obtains in the interaction picture

$$\frac{d\tilde{P}_{12}(t)}{dt}+\frac{i}{\hbar}\Delta\exp\{i[\bar{\omega}_{12}t-\frac{1}{\hbar}\int_0^t\mathbf{D}\cdot\mathbf{E}(t')dt']\}(P_{11}-P_{22}) = -\tilde{P}_{12}(\Gamma_{vL,1}+\Gamma_{cL,1}+\Gamma_{vL,2}+\Gamma_{cL,2}). \qquad (55)$$

Using next the expansion (24), and isolating the resonance terms, we finally find,

$$\frac{d\tilde{P}_{12}(t)}{dt}+\tilde{P}_{12}(\Gamma_{vL,1}+\Gamma_{cL,1}+\Gamma_{vL,2}+\Gamma_{cL,2}) = \frac{i}{\hbar}\Delta J_0(z)(P_{22}-P_{11})\exp(i\bar{\omega}_{12}t) \qquad (56)$$

and

$$P_{12}=\tilde{P}_{12}J_0(z)\exp(-i\bar{\omega}_{12}t) \qquad (57)$$

where

$$z=\frac{\mathbf{D}\cdot\mathbf{E}_0}{\hbar\omega} \qquad (58)$$

5.1. An analytically soluble model

The set of first order differential Eqs. (52) and (56) can be readily integrated, giving, for $P_{nn}(0)=P_{12}(0)=0$ and excitation by a rectangular pulse of duration t_p,

$$I(t)=\frac{e\Delta^2J_0^2(z)J_1^2(z_2)\gamma^{11}_{vR,2}}{\Delta^2J_0^2(z)+(\hbar^2/4)(\Gamma_{L1}+\Gamma_{R2})^2} \times\left\{1-\exp[-(\Gamma_{L1}+\Gamma_{R2})t]\cos\left[\frac{2}{\hbar}\Delta J_0(z)t\right]\right\}, \qquad (59)$$

where

$$\Gamma_{L1}=\Gamma_{vL,1}+\Gamma_{cL,1},\Gamma_{R2}=\Gamma_{vR,2}+\Gamma_{cR,2} \qquad (60)$$

denote the rates of electron transfer between molecular state $j = 1, 2$ and the corresponding lead, we used Eqs. (53) and (57) and put $\bar{\omega}_{12}=0$ for simplicity. In deriving Eq. (??), (59) we assumed that the spectral functions of r-th order for a given band are equal for the left and right contacts, i.e.,

$$\gamma^{rr}_{cL,i}=\gamma^{rr}_{cR,j} \text{ and } \gamma^{rr}_{vR,i}=\gamma^{rr}_{vL,j} \qquad (61)$$

for $i \neq j$ when $|r| > 1$, and that (as above)

$$\gamma^{11}_{vR,2}=\gamma^{-1,-1}_{cL,1}. \qquad (62)$$

In particular, as discussed before, the former assumption is expected to hold due to symmetry in the case of broad conduction and valance bands. When the relations given by Eqs. (61) and (62) are realized, the rates of electron transfer Γ_{L1} and Γ_{R2} are equal

$$\Gamma_{L1}=\Gamma_{R2} \qquad (63)$$

A plot of $I(t)$ versus time is shown in Figure 5. One can see that the current starts at zero and, at short time grows exponentially at a rate determined by the tunneling lifetime, $(\Gamma_{L1}+\Gamma_{R2})^{-1}$. In the long time limit the current approaches its steady-state value,

$$I_{SS}=\frac{e\Delta^2J_0^2(z)J_1^2(z_2)\gamma^{11}_{vR,2}}{\Delta^2J_0^2(z)+(\hbar^2/4)(\Gamma_{L1}+\Gamma_{R2})^2}, \qquad (64)$$

the first term on the right-hand side of Eq. (59). Most interestingly, at intermediate times $I(t)$ oscillates with frequency $\frac{2}{\hbar}\Delta J_0(z)$. The oscillation decays exponentially according to the tunneling lifetime $(\Gamma_{L1}+\Gamma_{R2})^{-1}$. Eq. (59) illustrates also the possibility of generating unidirectional current at times short with respect to $(\Gamma_{L1}+\Gamma_{R2})^{-1}$.

5.2. Coherent destruction of induced tunneling for the two-site case.

The steady-state current for a two-site molecular bridge, Eq. (64), is proportional to the square of the product of zero- and first-order Bessel functions $J_0(z)J_1(z_2)$ of different arguments z and $z_2=-z/2$. Consequently, the current vanishes at zeros of both $J_0(z)$ and $J_1(-z/2)$ (i.e., for the values of $|z| = 0, 2.4, 5.52, 7.6, 8.65, \ldots$). Thus, the phenomenon of CDIT for a two-site molecular bridge differs qualitatively from both CDIT for a single site bridge and the conventional CDT. In particular, for the 2-site bridge, both the coupling of the molecular bridge with semiconductor leads $V_{c(v)kj}$ and the electron hopping matrix element Δ are replaced through the interaction with the light by their effective values, $V_{c(v)kj} \to (V_{c(v)kj})_{eff} = J_{\mp1}(z_j)V_{c(v)kj}$ and $\Delta \to \Delta_{eff} = J_0(z)\Delta$ (see Eq. (64)). The corresponding effective tunneling matrix elements $(V_{c,vkj})_{eff}$ and Δ_{eff} vanish at zeros of $J_{\mp1}(z_j)$ and $J_0(z)$, respectively.

To determine the steady-state current versus z, Eq. (64), one needs to know z-dependence of $\Gamma_{L1}+\Gamma_{R2}$, which requires calculation of the rates $\gamma^{rr}_{c,vKj}$, Eq. (28), as functions of r, the order of the photonic replication. To evaluate $\gamma^{rr}_{c,vKj}$, it is useful to convert the sum over k in Eq. (28) into an integral over the energy $\varepsilon_{c,v}$, $\sum_k=\int_0^\infty d\varepsilon\rho^{(3)}(\varepsilon)$, where $\rho^{(3)}(\varepsilon_{c,v})$ is the density of states of the 3D semiconductor. This yields,

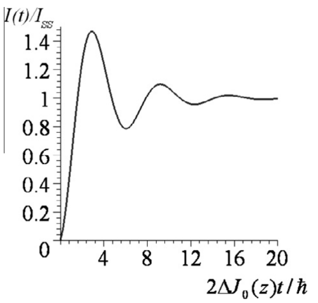

Figure 5. Current $I(t)$ versus time for two-site bridge when $\hbar(\Gamma_{L1}+\Gamma_{R2})=0.5\Delta J_0(z)$. I_{SS} denotes the steady-state value of $I(t)$, Eq. (64).

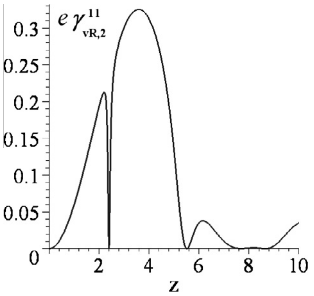

Figure 6. Steady-state current for two-site bridge versus z, calculated using Eqs. (64) and (67) for $\gamma^{22}_{vR,2} + \gamma^{-2,-2}_{cR,2} = 10\gamma^{11}_{vR,2}$ and $\hbar\gamma^{11}_{vR,2}/|\Delta| = 0.054$.

$$\begin{aligned}\gamma^{rr}_{c,vK_j,j} &= \frac{\pi}{\hbar}\int_0^\infty d\varepsilon_{c,v}\rho^{(3)}(\varepsilon_{c,v})|V_{c,vj}(\varepsilon_{c,v})|^2\delta(\varepsilon_{c,v} - \hbar\omega_j + r\hbar\omega) \\ &= \frac{\pi}{\hbar}|V_{c,vj}(\hbar\omega_j - r\hbar\omega)|^2\rho^{(3)}(\hbar\omega_j - r\hbar\omega)\end{aligned} \tag{65}$$

Bearing in mind that $\rho^{(3)}(\varepsilon_{c,v}) \sim \sqrt{\varepsilon_{c,v}}$[33], and neglecting the energy dependence of the tunneling matrix element $V_{c,vj}(\varepsilon_{c,v})$, one obtains for $|r| \geqslant 2$

$$\gamma^{rr}_{c,vK_j,j} = \sqrt{|r|-1}\,\gamma^{\mp2,\mp2}_{c,vK_j,j}, \tag{66}$$

with which

$$\Gamma_{R2} = \Gamma_{L1} = J_1^2(z/2)\gamma^{11}_{vR,2} + (\gamma^{22}_{vR,2} + \gamma^{-2,-2}_{cR,2})\sum_{r=2}^{\infty} J_r^2(z/2)\sqrt{r-1}, \tag{67}$$

where we used Eqs. (27), (61), (62) and (63). A plot of I_{SS} versus z is provided in Figure 6, illustrating that the steady-state current for the two-site bridge vanishes at both the zeros of the current corresponding to CDT and the zeros of the induced current for a single site bridge. We note also the qualitative difference between the currents for the single- and the double-site bridges, originating from the differences of the underlying electronic dynamics.

6. Conclusions

In the previous sections, we proposed a viable approach to coherent control of electric transport via molecular junctions and developed a theoretical framework to explore the method. Our approach makes use of semiconducting electrodes and sub-bandgap frequencies to circumvent substrate-mediated processes and competing energy transfer events. It relies on a simple and general concept, namely the controllable photonic replication of molecular levels through interaction of the molecular permanent dipole vector with an electromagnetic field. By exploring simple, analytically soluble limits for a single and two-site molecular bridge, we showed that, acting in conjunction with the bias voltage, the electromagnetic field induces unidirectional current in the junction, whose rate is determined primarily by the bias voltage while its temporal characteristics are controlled by the laser pulse. Our results show that photoinduced, unidirectional current is obtained for both a symmetric and an asymmetric position of a molecular orbital with respect to the CB and VB of the SC leads, giving evidence to the generality and the robustness of the proposed approach. We also predicted the phenomenon of coherent destruction of induced tunneling (CDIT), which extends the previously observed effect of coherent destruction of tunnelling (CDT). CDIT for a two-site bridge differs qualitatively from both CDT and from CDIT in a single site bridge, reflecting rather different dynamics of the electrons in the molecular wire in these two cases.

It is clear that opportunities for future research that will extend the simple models presented here are many and intriguing. Numerical application of the theory developed in Section 3 that will include multiple sites and account for nonMarkovian effects would provide general insights into the role of nonMarkovian physics in light controlled junctions and the extent to which the effects observed analytically here survive in the realistic many-site case. Likewise instructive would be an extension of our model to realistic molecular bridges, e.g., oligophenylene molecules with varying numbers of phenyl rings. The photoconductance of such molecular bridges attached between two metallic electrodes and subject to monochromatic light irradiation was studied in Refs. [34,35]. Both the exploration of the multiple-site, nonMarkovian problem and the extension of our method to treat a realistic molecular bridge are the topics of ongoing research in our group.

Other approaches to optical control of transport via junctions, which similarly take advantage of the band gap of semiconductors and sub-bandgap frequencies, could be readily envisioned. The approach introduced in Ref. [13], where the concept of nonadiabatic alignment is utilized to introduce a nanoscale, ultrafast switch, could be generalized through application of the recently developed torsional control approach [36,37]. Here, a circularly- or an elliptically-polarized, low frequency laser pulse is applied to transiently force a nonrigid, twisted molecule (as, e.g., a biphenyl derivative) into coplanarity, with a dramatic effect on the optical as well as the electronic properties of the system. When a molecule of this gender is connected to semiconductor electrodes and subjected to an appropriately polarized, sub-bandgap laser pulse, the resulting molecular junction is expected to exhibit a conductance on–off ratio of ca. one and a half orders of magnitude along with sub-picosecond conductance on–off time scales. Likewise, the method of resonant chirped pulse excitation of a molecular optical transition, previously applied (with several undesired competing effects) to metal-based molecular junctions, could benefit from the introduction of SC-based junctions, potentially enabling us to maximize photoinduced current through a junction due to adiabatic rapid passage. A theory to model this method for metallic contacts and a molecular bridge characterized by a strong charge-transfer transition into the first excited state [38] has been developed in Refs.[4,5]. The use of SC contacts will enable realization of a coherent version of the method, specifically, the transfer of electron charge e per optical pulse (see Eq. (61) of Ref. [4] and the corresponding discussion). This opportunity may find application in the development of single-electron devices with optical gating based on molecular nanojunctions. These and other avenues of extending coherent control concepts and tools to the domain of molecular junctions will be the topic of future research.

Acknowledgements

B.D.F. gratefully acknowledges support by the US-Israel Binational Science Foundation (Grant No. 2008282) and the Northwestern-Tel Aviv University Exchange Program for support of a visit to Northwestern University, in the framework of which this research was carried out. T.S. is grateful to the National Science Foundation (Grant No. CHE-1012207) and the US Department of Energy (Grant No. DE-FG02–09ER16109) for support.

References

[1] F. Chen, N.J. Tao, Acc. Chem. Res. 42 (2009) 429.
[2] J.R. Heath, Annu. Rev. Mater. Res. 39 (2009) 1.
[3] S. Kohler, J. Lehmann, P. Hanggi, Phys. Rep. 406 (2005) 379.
[4] B.D. Fainberg, M. Jouravlev, A. Nitzan, Phys. Rev. B 76 (2007) 245329.
[5] B.D. Fainberg, M. Sukharev, T.-H. Park, M. Galperin, Phys. Rev. B 83 (2011) 205425.
[6] M. Galperin, S. Tretiak, J. Chem. Phys. 128 (2008) 124705.
[7] R. Haertle, R. Volkovich, M. Thoss, J. Chem. Phys. 133 (2010) 081102.
[8] U. Kleinekathofer, G. Li, S. Welack, M. Schreiber, Europhys. Lett. 79 (2007) 27006.
[9] G. Li, M. Schreiber, U. Kleinekathoefer, New J. Phys. 10 (2008) 085005.
[10] G. Li, M. Schreiber, U. Kleinekathoefer, Phys. Status Solidi B 245 (2008) 2720.
[11] T.-H. Park, M. Galperin, Phys. Rev. B 84 (2011) 075447.

[12] A. Prociuk, B.D. Dunietz, Phys. Rev. B 78 (2008) 165112.
[13] M.G. Reuter, M. Sukharev, T. Seideman, Phys. Rev. Lett. 101 (2008) 208303.
[14] I. Thanopulos, E. Paspalakis, V. Yannopapas, Nanotechnology 19 (2008) 445202.
[15] L. Wang, V. May, Phys. Chem. Chem. Phys. 13 (2011) 8755.
[16] B. Fainberg, A. Nitzan, Phys. Status Solidi A 206 (2009) 948.
[17] A. Zrenner, E. Beham, S. Stufler, F. Findeis, M. Bichler, G. Abstreiter, Nature 418 (2002) 612.
[18] V.L. Bogdanov, B.D. Fainberg, Opt. Spectrosc. 41 (1976) 472 (Opt. Spektrosk. 41 (1976) 799).
[19] B.D. Fainberg, Opt. Spectrosc. 41 (1976) 558 (Opt. Spektrosk. 41 (1976) 944).
[20] B.D. Fainberg, Opt. Spectrosc. 41 (1976) 228 (Opt. Spektrosk. 41 (1976) 397).
[21] B.D. Fainberg, V.A. Gorbunov, S.H. Lin, Chem. Phys. 307 (2004) 77.
[22] P. Hanggi, S. Kohler, J. Lehmann, M. Strass, in: G. Cuniberti, G. Fagas, K. Richter (Eds.), Introducing Molecular Electronics, Springer-Verlag, Berlin, Heidelberg, New York, 2005, p. 55.
[23] G. Li, B.D. Fainberg, A. Nitzan, S. Kohler, P. Hanggi, Phys. Rev. B 81 (2010) 165310.
[24] S. Welack, M. Schreiber, U. Kleinekathofer, J. Chem. Phys. 124 (2006) 044712.
[25] B. Fainberg, T. Seideman, Phys. Status Solidi A 209 (2012) 2433.
[26] F. Grossmann, T. Dittrich, P. Jung, P. Hanggi, Phys. Rev. Lett. 67 (1991) 516.
[27] F. Grossmann, P. Hanggi, Europhys. Lett. 18 (1992) 571.
[28] U. Kleinekathofer, G. Li, S. Welack, M. Schreiber, Europhys. Lett. 75 (2006) 139.
[29] J. Lehmann, S. Camalet, S. Kohler, P. Hanggi, Chem. Phys. Lett. 368 (2003) 282.
[30] G. Li, U. Kleinekathofer, M. Schreiber, J. Lumin. 128 (2008) 1078.
[31] M. Abramowitz, I. Stegun, Handbook on Mathematical Functions, Dover, New York, 1964.
[32] U. Harbola, S. Mukamel, J. Chem. Phys. 124 (2006) 044106.
[33] H. Haug, S.W. Koch, Quantum Theory of the Optical and Electronic Properties of Semiconductors, World Scientific, Singapore, 2001.
[34] J.K. Viljas, F. Pauly, J.C. Cuevas, Phys. Rev. B 76 (2007) 033403.
[35] J.K. Viljas, F. Pauly, J.C. Cuevas, Phys. Rev. B 77 (2008) 155119.
[36] S.M. Parker, M.A. Ratner, T. Seideman, J. Chem. Phys. 135 (2011) 224301.
[37] S. Ramakrishna, T. Seideman, Phys. Rev. Lett. 99 (2007) 103001.
[38] M. Galperin, A. Nitzan, Phys. Rev. Lett. 95 (2005) 206802.

Boris D. Fainberg received his Ph.D. degree (1977) from the State Optical Institute named for S.I. Vavilov (St.-Petersburg, Russia) where he was employed as a research associate, senior research associate and associate professor in the department of molecular spectroscopy (till 1990). In 1991 he moved to the School of Chemistry at Tel-Aviv University where he worked as a research associate (till 1998) and then as a visiting professor beginning 2000. In 1998 he joined the staff of the faculty of sciences of the Holon Institute of Technology (Holon, Israel) as an associate professor and then (2003) as a professor of chemical physics. He was a visiting professor at Institute of Atomic and Molecular Science, Taipei, Taiwan (2000), Institute of Physics and Chemistry of Materials, CNRS, Strasbourg (2001 and 2002), Humboldt University of Berlin (2003), University of Augsburg (2007), Northwestern University, Evanston, IL (2011 and 2012). His research interests include non-Markovian effects in four-photon spectroscopy, coherent optical control, molecular electronics, nanophotonics and plasmonics.

Tamar Seideman received a Ph.D. in 1990 from the Weizmann Institute of Science, Israel, and continued to postdoctoral research in UC Berkeley as a Weizmann Fellow and a Fulbright Fellow, taking a faculty position at the National Research Council of Canada, Ottawa in 1992. Since 2003 she has been a Professor of Chemistry at Northwestern University and since 2004 a Professor of Chemistry and Physics. Her research has been recognized with numerous awards, including a Sackelr Award, a senior A. von Humboldt Award, a Weston Award, an Emerson Award, a Brener award, and a J.F. Kennedy award. She is a member of the National Academy of Science of Germany, a Fellow of the American Physical Society, a Guggenheim Fellow, and the author of 204 publications. Among Seideman's research interests are (1) quantum transport, molecular electronics, current-driven nanochemistry and molecular machines; (2) ultrafast nanoplasmonics and information guidance in the nanoscale; (3) coherent control and coherence spectroscopies in isolated molecules and in dissipative media; (4) attosecond science and the interaction of matter with intense laser fields; (5) photomanipulation of external and internal molecular modes; and (6) mathematical method development.